IOP Conference Series: Earth and Environmental Science

PAPER • **OPEN ACCESS**

Roll-up region of tip vortex: numerical investigation

To cite this article: M Reclari *et al* 2019 *IOP Conf. Ser.: Earth Environ. Sci.* **240** 072027

View the article online for updates and enhancements.

This content was downloaded from IP address 128.178.141.172 on 08/09/2020 at 07:50

Roll-up region of tip vortex: numerical investigation

M Reclari[1], T Sano[1], M Iino[1], M Dreyer[2], A Amini[2] and M Farhat[2]

[1] Mitsubishi Heavy Industries, Ltd., Research & Innovation Center, Hyogo Japan
[2] Laboratoire de Machines Hydrauliques, Ecole Polytechnique Fédérale de Lausanne, Avenue de Cour 33bis, 1007 Lausanne Switzerland

martino1_reclari@mhi.co.jp

Abstract. The appearance of gas-filled vortices at the tip of hydraulic machines blades is usually associated with increase of losses, vibrations, noise and erosion risk. The understanding of the roll-up region, where the boundary layer on the pressure side crosses the foil and generates the vortex on the suction side, is of primary importance to control the vortex behaviour. However, the very strong gradients encountered in the regions make numerical simulations and experimental measurements particularly challenging. In the present paper we study the roll-up region of a tip vortex on a skewed-back blade, comparing the results with experimental observations (position of the rollup region, cavitation number at cavitation inception) as well as with detailed velocity measurements, in order to identify the most appropriate computation settings. Using these settings we numerically investigate the role of the leading edge vortex and its interaction with the one generated at the tip.

1. Introduction

Finite-span wings, like the blades of propellers, axial pumps and turbines, generate a vortex at the tip of the lifting surface, as a direct consequence of the pressure difference between the pressure and suction sides. As the vortex is fed by the vorticity sheet generated by the wing, the pressure at its core drops [1]. If the pressure falls below the vapor pressure, the liquid may rupture and evaporate into a cavitation bubble. Gas-filled vortices are a key issue in many applications of hydraulic machines, since their presence is usually associated with increase of losses, vibrations, noise and erosion [2, 3]. However, due to the very strong gradients present in the phenomena, a correct prediction of the vortex structure is still challenging for numerical simulations. Strategies to obtain reliable estimations of the characteristics of free stream vortices include sophisticated turbulence models [4] and extensive refinement of mesh [5, 6, 7]. While these investigations mainly focus on the computation of free vortices, very little numerical simulations exist of the vortex roll-up region.

From an industrial application point of view, the roll-up region is important for several reasons: in elliptical hydrofoils the minimum pressure in the vortex line is expected very close to the tip of the foil [8]. Therefore, a mesh which is very fine in the wing tip region and coarser downstream will suffice to a correct prediction of the cavitation (although the path and strength of the vortex after it leaves the blade would be inaccurate). Moreover, most of the techniques to control the vortex and its cavitation behavior require an intervention in the wing tip region [9] in the roll-up region.

In the present study we systematically investigate the requirements, in terms of mesh and turbulence model, to obtain a reliable prediction of the wing tip region. The simulations are compared with experimental observations of cavitation inception and desinence, as well as with boundary layer

Content from this work may be used under the terms of the Creative Commons Attribution 3.0 licence. Any further distribution of this work must maintain attribution to the author(s) and the title of the work, journal citation and DOI.
Published under licence by IOP Publishing Ltd

measurements. Since the size of the vortex (and therefore its minimum pressure) is directly given by the thickness of the boundary layer during the roll-up process [10], correct prediction of the boundary layer is crucial. Once appropriate settings have been identified, the simulations are used to gain additional insight into the tip vortex roll-up region and its interaction with the leading edge vortex in a swept back hydrofoil.

2. Case study

The case presented in this paper is a single blade with elliptical skewed back planform and asymmetric profile, as shown in figure 1a. The asymmetric cross-section of this hydrofoil results in non-zero lift and consequently stable tip vortex from zero incidence. The case is investigated numerically and experimentally in order to obtain reliable CFD simulation and shed new light into the roll-up phenomena.

2.1. *Computational setup*

The computation is done in a rectangular box, with a velocity inlet, symmetry walls and pressure outlet boundary conditions. The dimensions of the box are given in figure 1b as a function of the wing chord. The working fluid is water, and since we are investigating the phenomena before cavitation inception, the simulation is single phase: no cavitation model is applied. The simulations are performed in steady state only with Ansys Fluent 16.2.

The mesh is unstructured, with boundary layer mesh applied to the foil walls, as shown in figure 2b. The region downstream of the blade is not refined to allow the vortex to diffuse (numerically), thus reducing the number of cells required. Moreover, the outlet boundary imposes the average pressure on the whole surface, without forcing a homogeneous pressure distribution. This also helps the exit of the vorticity that has not been dissipated.

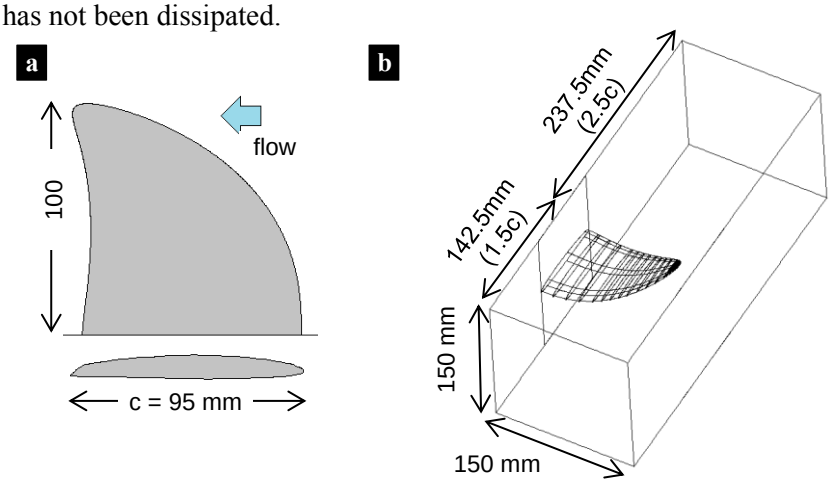

Figure 1. a. Planform (above) and profile (below) of the skewed back hydrofoil used as test case. **b.** Dimension of the computational domain.

Various spatial discretization (mesh) and turbulence models were used with this setup and compared with experimental results in order to determine the settings giving the most accurate predictions. An important parameter used to evaluate the quality of each simulation is the minimum pressure coefficient observed at the core of the vortex, defined as:

$$C_{p_{min}} = \frac{P_{min} - P_\infty}{\frac{1}{2}\rho V_\infty^2} \quad (1)$$

where ρ is the density of the liquid (in this case, water), P_∞ and V_∞ are the pressure and velocity of the free stream flow respectively, and P_{min} is the minimum pressure observed at the core of the vortex.

2.2. *Experimental setup*

The measurements on the blade have been performed at the LMH cavitation tunnel [11], having a test section of 150x150x750 mm. The cavitation map is investigated for a given incidence angle varying the pressure in the test section from a cavitation-free condition to reach the first appearance of cavitation (inception), then further reducing the pressure to obtain well-developed cavitation before increasing it back to cavitation free condition (desinence). To account for the complex cavitation physics, two criteria are used: the observation of intermittent cavitation along the vortex core, i.e. the occurrence of the first (inception), or last (desinence), cavitation bubble, and the occurrence of a permanent vapor core attached to the foil tip. These criteria are defined as *intermittent* and *established* respectively. The cavitation map is traditionally expressed in a dimensionless way using the cavitation coefficient:

$$\sigma = \frac{P_\infty - P_{vap}}{\frac{1}{2}\rho V_\infty^2} \quad (2)$$

where P_{vap} is the vaporization pressure of the liquid at the working temperature.

Moreover, the boundary layer on the hydrofoil has been measured using 2-component Laser Doppler Velocimetry (LDV) with 300 mm focal length lens, mounted on a traversing system with a resolution of 10 µm and using 20 µm polyamide tracking particles. The velocity measurement in the boundary layer is performed along a single line located 40 mm downstream of the foil center-line and 80 mm from the foil root in the span direction, as shown in figure 2 a. The boundary layer is measured over 22 points, located between 0 and 2mm above the foil suction surface; for each point at least 5000 Doppler bursts are averaged to evaluate the local mean velocity.

3. Results

In this section, we first detail the steps undertaken to obtain simulations results that are comparable with experimental observations. Then, the results from the simulation using the best setup are shown and discussed.

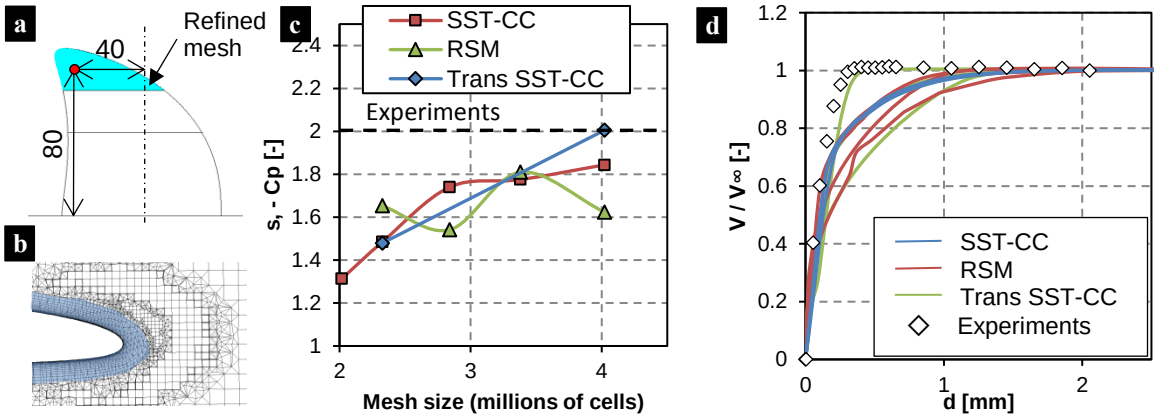

Figure 2. a. The location of the boundary layer measurement (red dot) and the region where the surface mesh is refined (highlighted in light blue). **b.** Detail of the leading edge showing the near-wall meshing strategy with several layers (highlighted in light blue). **c**. Comparison of experimental desinent cavitation number (black dashed line) and computation results (solid colour lines) as a function of the mesh size, for the different turbulence models. **d.** Experimental (black diamonds) and numerical (solid colour lines) velocity profiles of the suction side boundary layer as a function of the distance from the wall, for the various turbulence models.

3.1. *Validation of the CFD results*

In order to obtain reliable computational results, the test case was simulated using various combination of turbulence model and mesh qualities. Two Boussinesq hypothesis based turbulence models were

tested: the k-ω Shear Stress Transport with curvature correction (SST-CC) and the Transition SST, also with curvature correction (Trans SST-CC). Moreover, the Reynolds Stress Model (RSM), based on the transport of the instability terms in the turbulence stress tensor was also tested, in its linear pressure strain implementation.

All turbulence models use scalable wall functions to provide mesh-insensitive treatment of the near-wall region. The meshes tested differ in the quality of the surface mesh at the wing tip and the number and thickness of the mesh layers at the wall (see figure 2a and b).

In figure 2c the minimum pressure coefficient predicted by the CFD is compared with the observed desinent cavitation number as a function of the mesh size to assess the quality of the computations. The desinent cavitation number is chosen instead of the inception one because it has been shown that inception of cavitation largely depends on water quality, especially nuclei content [12, 13], and is therefore not adequate as precise pressure measurement. Moreover, detailed measurement of the vortex velocity profile in the near wake region demonstrated that the desinent cavitation number is a very good estimation of the minimum pressure within the vortex [14]. The transition model is the one which displays the highest pressure coefficient (therefore the lowest pressure inside the vortex) without using an excessively large mesh. It is interesting to note that the pressure coefficient predicted by the RSM model seems to be somehow unrelated to the mesh size. This suggests that the model is not very well suited for resolving simulation of boundary layer phenomena, while it has been proved to be able to predict well the free stream vortices [7].

The boundary layer velocity profiles measured on the foil suction side (see location in figure 2a), are compared with those computed by CFD in figure 2d. It is straightforward to observe that the only simulation that captures the laminar boundary layer as measured in the experiments is the Transition SST-CC model, when an appropriated near wall mesh is used. This corresponds to the mesh with nearly 4M cells that predicts C_p = -2 in figure 2c. Therefore, we believe that the principal reason for the good estimation of the minimum pressure of the vortex is correct prediction of the boundary layer.

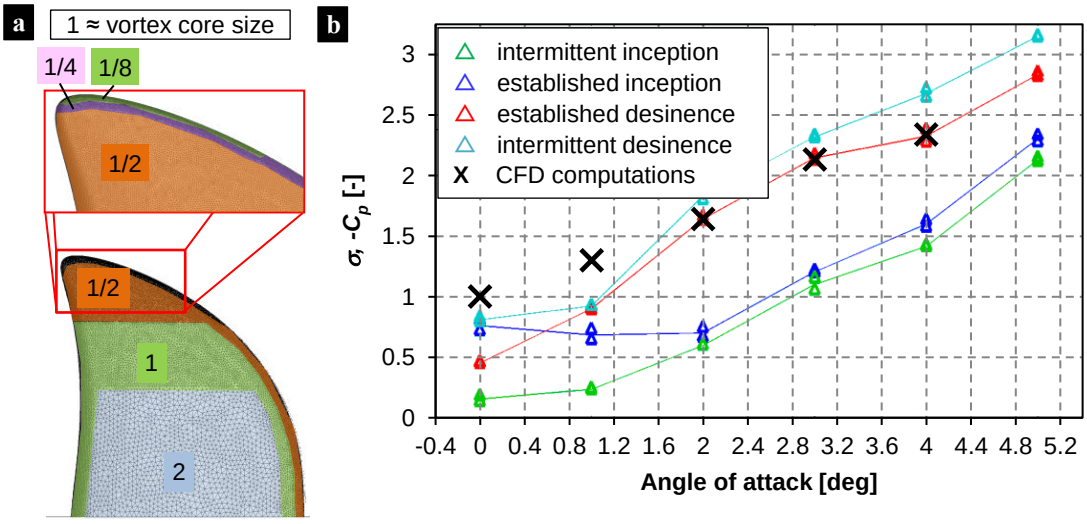

Figure 3. a. Refinement of the surface mesh on the foil, given as multiples of the estimated size of the viscous core of the vortex. **b.** Comparison between the minimum pressure coefficient (CFD, black crosses) and desinent cavitation number (experiments, colour triangles) as a function of the angle of attack, obtained with fully gas-saturated water.

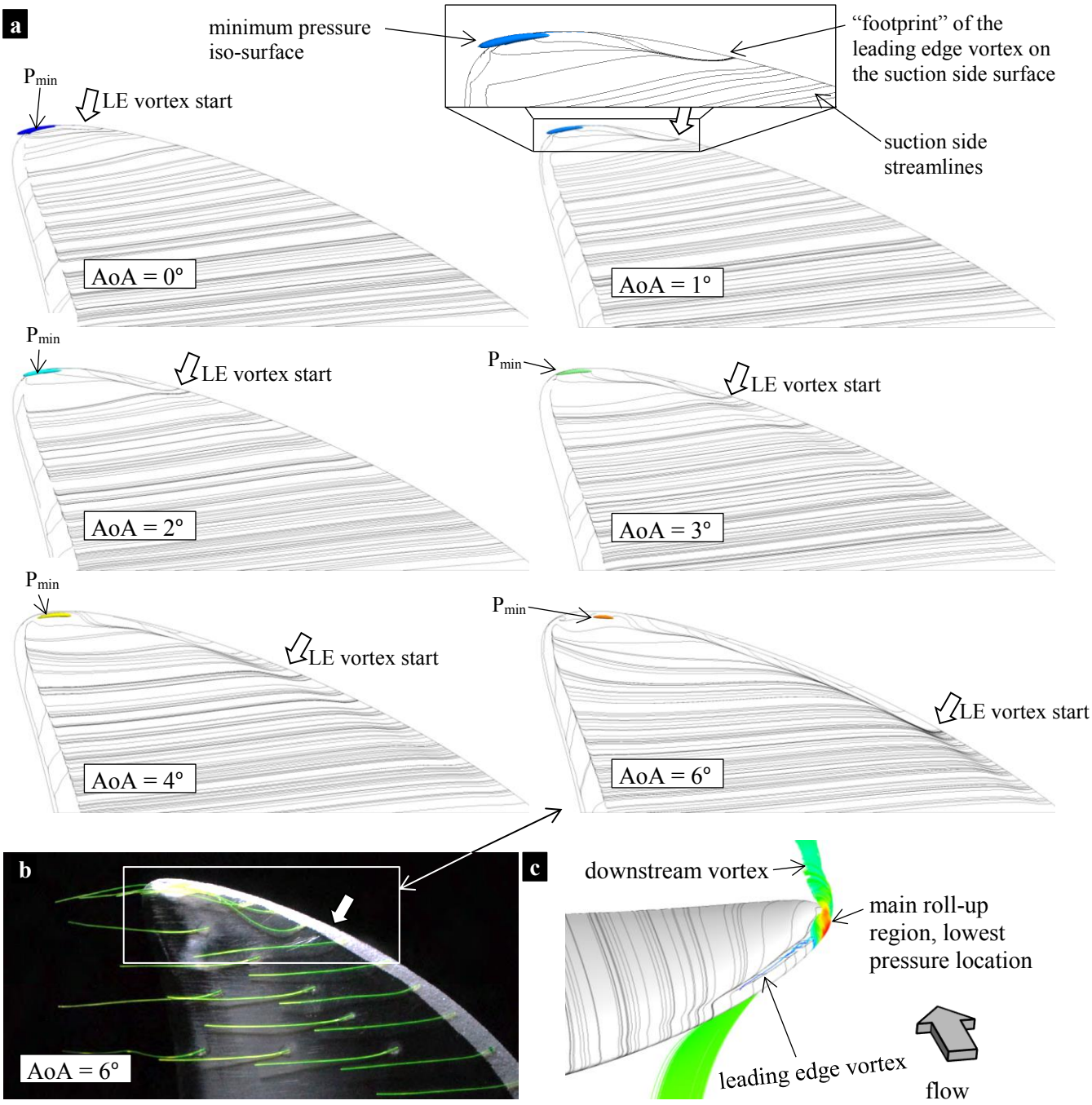

Figure 4. a. Streamlines on the suction sides and region of the minimum pressure (iso-surface 20kPa above the minimum pressure) for angles of attack from 0 to 6°. **b.** Example of experimental flow visualization with tufts, for an angle of attack of 6°. The leading edge vortex is clearly visible as the deformation of the tufts in the leading edge region. **c.** Detail of the wing tip region at 6° angle of attack as seen from upstream, with surface streamlines (thin black lines) and streamlines going through the minimum pressure region (the colour of the streamline defines the local flow velocity). While most of the flow feeding the roll-up comes from the pressure side,

From the previous observations, the SST transition model, together with the surface mesh quality shown in figure 3a, was used to investigate the behavior of the vortex. This mesh has a slightly different surface discretization than those used to assess the validity of the computation; it is more refined at the tip leading edge and coarser on the main surfaces of the blade. Also, particular care is taken when meshing the boundary layer: the mesh has up to 25 layers (at the wing tip) of prism elements, thus including the location of lowest pressure in the vortex core entirely in this finely refined region. This also ensures values of y^+ below 1 on the entire surface. Good agreement of the measured and predicted minimum pressure coefficients is observed over angles of attack above 1 degree, as shown in figure 3 b.

3.2. *Vortex behaviour*

In figure 4a are depicted the streamlines on the blade suction side, together with the location of the minimum pressure, for various angles of attack. A deformation of the surface streamlines near the leading edge is clearly visible: this is the "footprint" of the leading edge vortex, whose starting location (where the flow crosses from the pressure to the suction side) strongly depends on the angle of attack. This vortex is akin to the ones developed on the suction side of delta wings, where they are attached to the sharp leading edge. In the present case the rounded leading edge is thought to be responsible for the dependency of the vortex starting location on the angle of attack. Experiments performed using tuft to identify the footprint of the leading edge vortex have a very good agreement with the computations, as shown for an angle of attack of 6° in figure 4b.

Always in figure 4a, iso-surfaces are used to identify the regions around the minimum pressure obtained with each angle of attack, which is where the main roll-up of the tip vortex occurs. This region also moves upstream as the angle of attack is increased, although to a less extent than the footprint of the leading edge vortex. The leading edge vortex, being basically a recirculation region due to the crossing of the flow from the pressure to the suction side, has maximum velocities of the order of magnitude of the free stream velocity. On the other hand, the tip vortex is given by the circulation of the entire blade, and has therefore much larger maximum velocities. For this reason, it is not surprising that the location of the lowest pressure is the tip vortex. From there, the cavitation is thought to propagate into the leading edge vortex and downstream.

These two phenomena are typical of skewed back and propeller blades, and they cannot be treated as completely independent since the leading edge vortex transitions into the tip vortex at the tip of the blade. From the analysis of the streamlines going through the lowest pressure region (shown in figure 4c), it seems that the tip vortex core is mainly fed by flow crossing from the pressure side at the wing tip. However, some of the streamlines show that at least a small proportion of flow comes from the leading edge vortex.

4. Conclusions

In the present paper we have used numerical simulation to investigate the roll-up region of a tip vortex in a skewed back blade, and its interaction with the leading edge vortex. The numerical models and the spatial discretization have been compare with experimental measurement to determine that the Transition SST turbulence model (with curvature correction) coupled with a very fine mesh in the wing tip region correctly predicts the minimum pressure at the vortex core. This is thought to be related to the model's ability to correctly capture the boundary layer velocity distribution. The simulations obtained with this setup show that while the leading edge vortex roll-up region moved upstream as the angle of attack is increased (as observed in experiments), the roll-up of the tip vortex and the lowest pressure region are only slightly affected. Since the tip vortex roll-up region is only slightly affected by the starting location of the leading edge vortex, we believe that strategies to control the tip vortex cavitation acting on the wing tip can be successful over a wide range of angles of attack.

References

[1] B. W. McCormick Jr, "On cavitation produced by a vortex trailing from a lifting surface," *Journal of Basic Engineering,* vol. 84, pp. 369-379, 1962.

[2] R. E. A. Arndt, "Cavitation in fluid machinery and hydraulic structures," *Annual Review of Fluid Mechanics,* vol. 13, no. 1, pp. 273-326., 1981.

[3] R. E. A. Arndt, "Cavitation in vortical flows," *Annual review of fluid mechanics,* vol. 34, no. 1, pp. 143-175, 2002.

[4] T. Frank, C. Lifante, S. Jebauer, M. Kuntz and K. Rieck, "CFD Simulation of Cloud and Tip Vortex Cavitation on Hydrofoils," in *Proceedings of the 6th International Conference on Multiphase Flow*, Leipzig (Germany), 2007.

[5] N. Kasmai, D. Thompson, E. Luke, M. Jankun-Kelly and R. Machiraju, "Feature-based adaptive mesh refinement for wingtip vortices," *International Journal for Numerical Methods in Fluids,* vol. 66, no. 10, pp. 1274-1294, 2010.

[6] M. Dindar, A. Z. Lemnios, M. S. Shephard, J. E. Flaherty and K. Jansen, "An adaptive solution procedure for rotorcraft aerodynamics," *AIAA paper,* vol. 98, p. 2417, 1998.

[7] M. Reclari, S. Fukao, I. M. T. Sano and Y. Nakamura, "CFD of Vortical Flows: Requirements and Mesh Adaption Techniques," in *ASME/JSME/KSME 2015 Joint Fluids Engineering Conference. American Society of Mechanical Engineers*, Seoul, 2015.

[8] J. A. Astolfi, D. H. Fruman and J. Y. Billard, "(1999). A model for tip vortex roll-up in the near field region of three-dimensional foils and the prediction of cavitation onset," *European Journal of Mechanics-B / Fluids,* vol. 18, no. 4, pp. 757-775, 1999.

[9] G. P. Platzer and W. G. Souders, "Tip vortex cavitation characteristics and delay on a three-dimensional hydrofoil," in *19th American Towing Tank Conference*, 1980.

[10] D. Fruman, C. Dugué, A. Pauchet, P. Cerrutti and L. Briançon-Marjollet, "Tip vortex roll-up and cavitation," in *19th Symposium on Naval Hydrodynamics*, Seoul, 1992.

[11] M. Dreyer, J. Decaix, C. Münch-Alligné and M. Farhat, “Mind the gap: a new insight into the tip leakage vortex using stereo-PIV,” *Experiments in Fluids,* vol. 55, no. 11, pp. 1-13, 2014.

[12] R. E. Arndt and A. P. Keller, "Water quality effects on cavitation inception in a trailing vortex," *Journal of fluids engineering,* vol. 114, no. 3, pp. 430-438, 1992.

[13] R. E. Arndt, "Recent advances in cavitation research," *Advances in Hydroscience,* vol. 12, pp. 1-78, 1981.

[14] D. H. Fruman, P. Cerrutti, T. Pichon and P. Dupont, "Effect of hydrofoil planform on tip vortex roll-up and cavitation," *Journal of fluids engineering,* vol. 117, no. 1, pp. 162-169., 1995.